The Wind Retrieval Using Bistatic Doppler Radar and Its Precision Investigated

Mo Yueqin[1, 2)], Liu Liping[2)] and Xu Baoxiang[2)]
[1)] Meteorological Observation Center CMA, 100081,China
Tel.8610-68408740, Fax.8610-68408949, E-mail moyq@sohu.com
2) State Key Laboratory of Severe Weather Chinese Academy of Meteorological Sciences

Abstract

On the basis of multiple Doppler wind retrieval, a scheme is developed for C-band bistatic Doppler wind retrieval through a wind vector compositing technique, with an algorithm for 3D and 2D wind retrieval from observations of one transmitter(T)-two bistatic receiver(R) and one transmitter(T)-one bistatic receiver(R) (denoted as 1T2R and 1T1R). Numerical simulation of the 2D wind algorithm show it to be feasible. The precision of 2D and 3D wind retrieval has been simulated, deriving that when the 1T2R network is arranged as an equilateral triangle, the horizontal wind retrieval errors are distributed in an egg-like shape and when 1T2R network is positioned as an isosceles triangle with the base longer compared to one of the other sides and the transmitter at the apex, we can properly expand the retrieval domain. It is also found that the error distribution for the bistatic (1T1R) radar retrieval is similar to that for a two single radar network, except for smaller area of retrieval. The observation-based 2D wind retrieval and analysis lead to expected results. The research shows that bistatic probings can serve as a good supplement to single-radar detection, particularly where investment is not too high, in which case the use of the principle of bistatic lateral probing would remedy some deficits of single radar probing, resulting in a still higher output – input ratio with respect to a network of multiple single-base radars.

1. Introduction

The Doppler weather radar is an important tool in atmospheric sounding as well as research into physics of clouds and precipitation, and is thus widely applied to atmospheric studies, weather forecasting and warning both in theoretical and operational aspects. In the scope of radar meteorology, a range of atmospheric wind retrieval techniques has been developed by investigators during their long-term activities. However, the character of the wind field and certain simplifications to be done of complicated models in deriving 3D winds makes these applied techniques showing restraints and hence applicability only in certain cases, resulting in their limited applications.

To remove effects of the assumptions, more than two single Doppler radars are operated together to obtain radial velocities of a target in multiple directions in an effort to directly acquire a 3D wind field structure as a technique that has been utilized in mesoscale field probing experiments (Ray et al., 1980; Qiu and Xu, 1996; Zhou and Wang, 2003), leading to quite satisfactory results. Nevertheless, it is hard to synchronously get radial velocities of a target in multiple directions by using more than two single-radars and the related observational errors would cause inaccurate retrieval of the wind field. Now, the quest for the bistatic Doppler radar applications provides us with a new approach.

The bistatic network includes one conventional Doppler weather radar and one or more remote passive receiver(s) with low-gain antenna(s). The former and the latter are respectively called transmitter and bistatic passive receiver. Lateral electromagnetic radiation of the scattering, which is derived from the beam emitted by the transmitter and then scattered by the meteorological target, are detected by the bistatic receivers, meanwhile the backscattering is detected by the transmitter itself. Based on synchronism of time and frequency it is possible to get Doppler velocities of the same target (scatterer) in different directions, thereby re-constructing a 2D or 3D wind field. The

bistatic radar network is capable of sounding radial velocity in different directions on a simultaneous basis, making fast scanning of precipitation systems and decreasing the wind probing errors resulting from the development of the detected rainfall system *per se* compared to the operation of multiple-radars working together at the same time.

A network of Doppler weather radars is presently under construction in China, of which the bistatic radar network may be an innegligible component, hence its detection deserves in-depth research. Theoretical quest and preliminary practice show that the bistatic technique is of great value to the improvement of wind retrieval precision and the warning of severe weather events and particularly to some special cases such as prediction of local severe weather, aviation security and weather modification and so on, bistatic network is promising prospect.

Study on bistatic Doppler radar network began early in western countries, which was employed to probe meteorological echoes as far back as the 1960s, followed by contributions of researchers (e.g., Atlas et al., 1968; Doviak and Weil, 1972). In 1993 sample machine of this technique which was developed by NCAR marks research of the bistatic radar in meteorological sounding scope actually reaches its new climax. This network was operated multi-fold in different places in the US (Wurman et al., 1993) to make exploratory research into the location of radar echo, time delay between detection at a bistatic receiver(R) of direct radiation from transmitter(T), Doppler frequency shift and wind retrieval. The advantages and applicability of the network was discussed, and also its inherent drawbacks and approaches to their overcoming. Result suggests that the bistatic radar technology is of practical usefulness.

Chinese radar-meteorologists made a substantial amount of efforts on the study of application of single Doppler radar network (Liu et al., 2005; Xu et al., 2000) and also made in-depth research on wind retrieval from dual-/tri-Doppler measurements, 3D dynamic structure of rainstorms, and error distribution of wind retrieval for a tri-Doppler radars network and their optimal deployment (Kong et al., 1994; Zhou and Zhang, 2002; Liu et al., 2003). However, the problem of the bistatic radar retrieval study began quite late. In addition to military purposes, the first atmospheric observation by a bistatc multiple-Doppler radar in China was operated for National Research Project, “Mechanisms and Prediction Theory of Disastrous Weather over China”, which facility was provided by Japan in 2002-2003. Subsequently, related studies were carried out in Nanjing University of Information Science and Technology as well as the Institute of Atmospheric Physics, Chinese Academy of Sciencer.

Anhui Sun-Create Electron Joint-stock Ltd led in the development of the bistatic Doppler radar network in China, which was put into experiment in May and November, 2004, separately, in Hefei region and derived the initial observations. To assist that study, Chinese Academy of Meteorological Sciences did analysis to the observation and developed a variational scheme for 3D wind retrieval (Liu et al., 2005) alongside more systematic study of sounding theory (Mo, 2005; Mo et al., 2005) performed. The sample machine is being operated on an official basis over Ma’anshan area under the joint efforts of Anhui Meteorological Bureau, and the data are expected to be compared with measurements of a network consisting of three single radars. Bistatic wind retrieval and its precision need careful analysis so as to put the network into operation as early as possible.

2. Wind retrieval establishment for a bistatic radar network

2.1 Wind retrieval using multi-radar observation

In making wind probing, multiple-Doppler radar in a network is able to detect radial velocities of a meteorological target in different directions, with which to retrieve the wind field. Armijo (1969) proposed first a network of equations for retrieving 3D wind structure in the Cartesian coordinates

based on data from dual- or tri-Doppler radar (Armijo, 1969), which were utilized in the study on severe storms. Subsequently, more than one meteorologist derived equations by dint of a wind composite scheme, which is solved directly for theoretical research or application.

The position of a target under sounding is given by azimuth and elevation angle of each of the radars involved, leading to the following equation via wind speed compositing (Ray et al., 1980)

$$V_{ri} = u \sin a_i \cos e_i + v \cos a_i \cos e_i + W \sin e_i \qquad (1)$$

with $i = 1,2,\cdots,n$, where *n* is a positive integer.

in which *u*, *v* and *W* denote the velocity components in respective directions of the coordinate axes (*x*, *y*, *z*), V_{ri} the i-th radar – detected radial speed of the scatterer and *a* and *e* the azimuth and elevation angle of the *i*-th radar with respect to the scatterer (0º in due north), respectively.

2.2 Doppler Shifts and Radial Velocities of a Bistatic Receiver

In bistatic research all problems are commonly practiced onto a bistatic plane (Skolnik, 2003), thereby a 3D space is transformed onto a 2D plane to make the bistatic problem simplify and make its features distinct.

As shown in Fig.1, T and R designate one transmitter and a bistatic receiver, in order, vector V represents the component of projection of target's velocity vector on the bistatic plane at an included angle (δ, positive in a counterclockwise sense) with the bisector of bistatic angle β, R_t/ R_r denotes the distance to the target reached by the transmitter/receiver and L is the length of base line between the T and R.

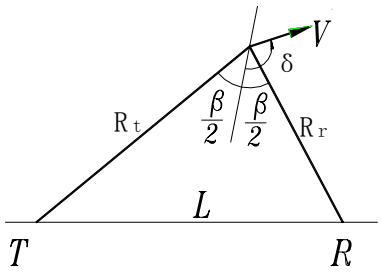

Fig.1. The velocity vector on a bistatic plane.

Doppler frequency shift caused by the target in movement in the bistatic network is given by (Yang et al., 2001)

$$f_B = \frac{V}{\lambda}[\cos(\delta + \frac{\beta}{2}) + \cos(\delta - \frac{\beta}{2})] = \frac{2V}{\lambda}\cos\delta\cos(\beta/2) \qquad (2)$$

With the bistatic angle β=0º, (2)-designated Doppler frequency shift becomes a problem for a single-base radar and β=180º denotes forward scattering.

In the bistatic detection the frequency shift is determined by the difference (in time elapsed) between path lengths (radiation from the transmitter to the receiver) from successive pulses. If the target were moving along the ellipse with the radars as focuses (or along its surface as in the 3D case, see Fig.2), then no phase change would be detected by the bistatic receiver, because the sum of distances from a point on the same ellipse to both the radars is equal, meaning zero difference in path between successive pulses. And for the receiver all points on the ellipse are viewed as equi-phase, so that transmitter and receiver are at focuses of the equi-phase ellipse. As a result, only the target moving perpendicularly to the ellipse can be detected, implying that in a real windfield, only when the velocity vector has non-zero projection component on the ellipse's normal line can the target (or scatterer) be detected by the bistatic receiver (Yang et al., 2001; Skolnik,

2003).

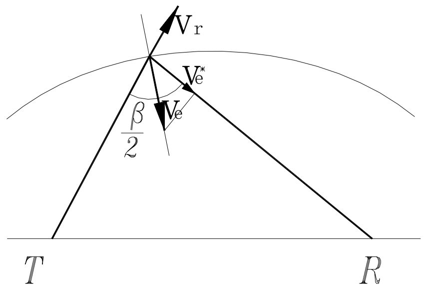

Fig.2. Geometry of Doppler velocity of bistatic receiver.

From (2) we know that the velocity measurement made by the bistatic radars is not equal to the projection of actual wind upon the bistatic angle bisector,but it is need to add a correction factor cos(β/2). By doing so, we have an expression of the velocity component (v_e) in the direction of the ellipse's normal of the form

$$v_e = \frac{v_e^*}{\cos(\beta/2)} \tag{3}$$

wherein v_e^* denotes the Doppler apparent speed measured by the bistatic receiver. Much attention should be directed to this expression in bistatic wind measurement and calculation.

2.3 Method Established for Wind Retrieval from Bistatic Receiver

By referring to the wind retrieval from multiple-Doppler radar, the method can be established by using a wind vector compositing scheme for the bistatic receivers. As stated earlier, the direction of passive receiver measured radial velocity is not the radial direction that radar beam moves but is perpendicular to an equi-phase surface of ellipse constituted by the transmitter and bistatic passive receiver as focuses, viz., in the direction of the normal line of the ellipse at an angle of (β/2) from the receiver antenna direction, that is, there is a difference by cos(β/2) between the passive receiver measurement and the projection component of actual wind on the ellipse normal line. As a result, after revising (1) we have the wind retrieval equation for the bistatic receivers. For a network of one transmitter and more than one bistatic receiver antenna, the equations are (Protat and Zawadzki, 1999; Wurman, et al., 1993), A and L.,

$$\begin{cases} V_{r1} = u\dfrac{\sin a_1 \cos e_1 + \sin a_t \cos e_t}{2\cos(\beta_1/2)} + v\dfrac{\cos a_1 \cos e_1 + \cos a_t \cos e_t}{2\cos(\beta_1/2)} + W\dfrac{\sin e_1 + \sin e_t}{2\cos(\beta_1/2)} \\ V_{r2} = u\dfrac{\sin a_2 \cos e_2 + \sin a_t \cos e_t}{2\cos(\beta_2/2)} + v\dfrac{\cos a_2 \cos e_2 + \cos a_t \cos e_t}{2\cos(\beta_2/2)} + W\dfrac{\sin e_2 + \sin e_t}{2\cos(\beta_2/2)} \\ \quad \ldots\ldots \\ V_{rn} = u\dfrac{\sin a_n \cos e_n + \sin a_t \cos e_t}{2\cos(\beta_n/2)} + v\dfrac{\cos a_n \cos e_n + \cos a_t \cos e_t}{2\cos(\beta_n/2)} + W\dfrac{\sin e_n + \sin e_t}{2\cos(\beta_n/2)} \\ V_{rt} = u\sin a_t \cos e_t + v\cos a_t \cos e_t + W\sin e_t \end{cases}$$

(with i=1, 2, …, n , where n is an integer) (4)

where symbols have the same meaning as in (1), that is, u, v and W signify the velocity components

of the target along coordinate axes x, y and z, in order; V_{r1}, V_{r2}, …, V_{rn} denote the 1st, 2nd , …, n-th passive-receiver-measured radial velocity perpendicular to the surface of the ellipse; a_1 and e_1, a_2 and e_2, …, a_n and e_n are the azimuth and elevation angle of the 1st, 2nd, …, n-th bistatic receiver relative to the scattering target respectively; V_{rt} stands for the radial velocity determined by the transmitter, with a_t and e_t giving the azimuth and elevation angle of the radar to the target, in order; β_1, β_2,……, β_n are the respective bistatic angle between the transmitter and bistatic receiver. Besides, the vertical speed of particle W is composed of vertical rising of air and its free falling velocity w_p with respect to air, suggesting that $W = w + w_p$.

2.4 The 3D Wind Structure and Algorithm to a Network of One transmitter and Two Bistatic Receivers (1T-2R)

To synchronously acquire radial velocity of the target in three directions, the bistatic radar generally comprises one transmitter and two passive receivers. Through the wind vector compositing we get the following equations

$$\begin{cases} V_{r1} = u\dfrac{\sin a_1 \cos e_1 + \sin a_t \cos e_t}{2\cos(\beta_1/2)} + v\dfrac{\cos a_1 \cos e_1 + \cos a_t \cos e_t}{2\cos(\beta_1/2)} + W\dfrac{\sin e_1 + \sin e_t}{2\cos(\beta_1/2)} \\ V_{r2} = u\dfrac{\sin a_2 \cos e_2 + \sin a_t \cos e_t}{2\cos(\beta_2/2)} + v\dfrac{\cos a_2 \cos e_2 + \cos a_t \cos e_t}{2\cos(\beta_2/2)} + W\dfrac{\sin e_2 + \sin e_t}{2\cos(\beta_2/2)} \\ V_{rt} = u\sin a_t \cos e_t + v\cos a_t \cos e_t + W\sin e_t \end{cases} \quad (5a)$$

parameters of (5a) are the same as in (4). Here (5a) are the linear equations with 3 unknown variables that are normally solved by a linear algebra method for winds u, v and W, whose coefficients are given as a, b and c for convenience, in order. Thus, (5a) are changed to

$$\begin{cases} a_1 u + b_1 v + c_1 W = V_{r1} \\ a_2 u + b_2 v + c_2 W = V_{r2} \\ a_3 u + b_3 v + c_3 W = V_{rt} \end{cases} \quad (5b)$$

By solving (5b), we have the forms of u, v and W as follows,

$$\begin{cases} u = (A_{11} * V_{r1} + A_{12} * V_{r2} + A_{13} * V_{rt})/A \\ v = (A_{21} * V_{r1} + A_{22} * V_{r2} + A_{23} * V_{rt})/A \\ W = (A_{31} * V_{r1} + A_{32} * V_{r2} + A_{33} * V_{rt})/A \end{cases} \quad (6)$$

in which

$$A = a_1 b_2 c_3 + a_2 b_3 c_1 + a_3 b_1 c_2 - a_1 b_3 c_2 - a_2 b_1 c_3 - a_3 b_2 c_1$$

$$A_{11} = b_2 c_3 - b_3 c_2 \qquad A_{12} = c_1 b_3 - b_1 c_3 \qquad A_{13} = b_1 c_2 - c_1 b_2$$

$$A_{21} = c_2 a_3 - a_2 c_3 \qquad A_{22} = a_1 c_3 - c_1 a_3 \qquad A_{23} = c_1 a_2 - a_1 c_2$$

$$A_{31} = a_2 b_3 - a_3 b_2 \qquad A_{32} = b_1 a_3 - a_1 b_3 \qquad A_{33} = a_1 b_2 - b_1 a_2$$

2.5 Estimation of Wind Retrieval Precision for a 1T-2R

For a 1T-2R the variance of wind compositing bears a relation to the relative position of the radars and also to the accuracy at which each of the radars measures the velocity. The expressions for estimating variance of u, v and W are

$$\sigma_u^2 = (A_{11}^2 \cdot \sigma_{r1}^2 + A_{12}^2 \cdot \sigma_{r2}^2 + A_{13}^2 \cdot \sigma_{rt}^2) / A^2 \quad (7)$$

$$\sigma_v^2 = (A_{21}^2 \cdot \sigma_{r1}^2 + A_{22}^2 \cdot \sigma_{r2}^2 + A_{23}^2 \cdot \sigma_{rt}^2) / A^2 \quad (8)$$

$$\sigma_w^2 = (A_{31}^2 \cdot \sigma_{r1}^2 + A_{32}^2 \cdot \sigma_{r2}^2 + A_{33}^2 \cdot \sigma_{rt}^2) / A^2 \quad (9)$$

with σ_{r1}, σ_{r2} and σ_{rt} denote the precision of velocity measurement of the respective radars.

With σ_{hor} representing the standard deviation of horizontal winds, the expression has the form

$$\sigma_{hor} = \sqrt{\sigma_u^2 + \sigma_v^2} \quad (10)$$

To visualize the space distribution of errors, a numerical modeling is performed. Assume the coordinates of the transmitter to be T (0, 0), the passive receiver (R1, 20 km away from T) to be R_1 (10, 20 sin 60°) and another (R2, 20 km away in the due east) to be R_2 (20, 0), all forming an equilateral triangle. Set the velocity measuring accuracy to be 1 m/s for all of them, and based on (10), we simulate and calculate the retrieval errors of bistatic horizontal winds, as shown in Fig.3 (a1 to a3) at 3 levels. Following the retrieval procedure for multi-radar operation, on the other hand, (1) is used to calculate wind retrieval errors for three single Doppler radars positioned as an equilateral triangle (Zhang et al., 1998), achieving the error distribution of horizontal wind retrieval at 3 levels shown in Fig.3 (b1 to b3).

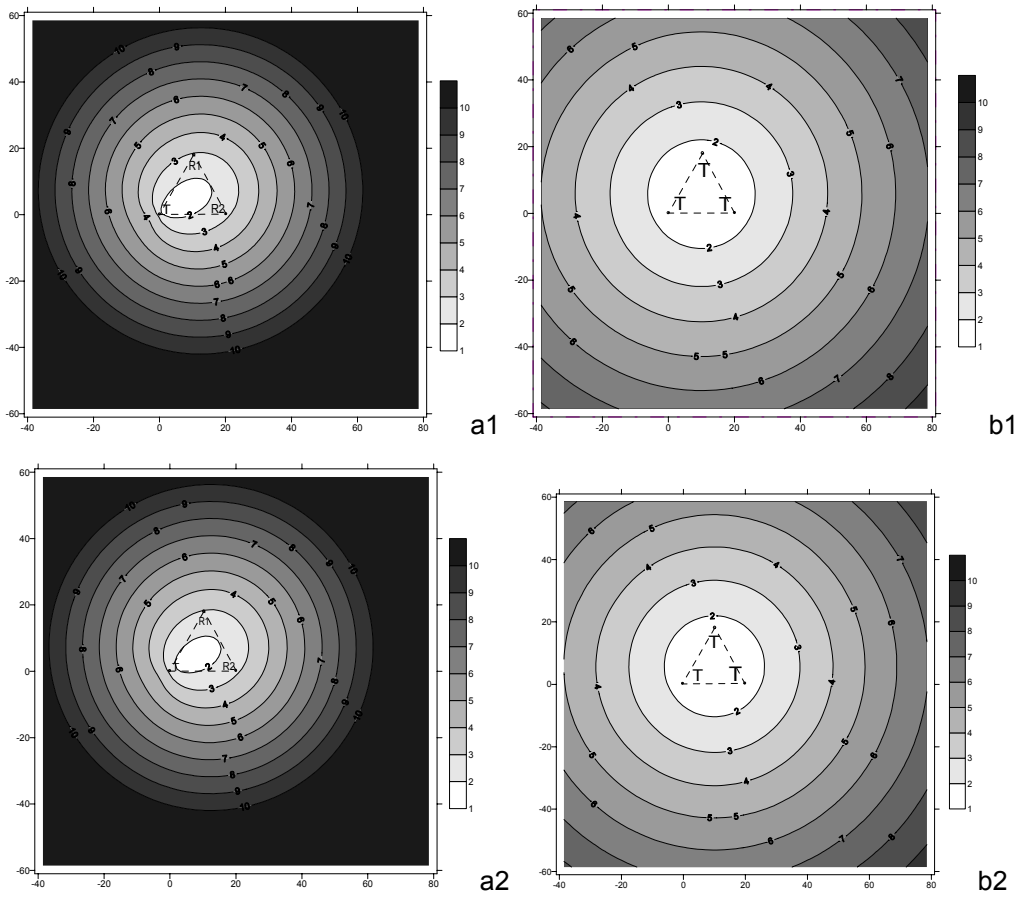

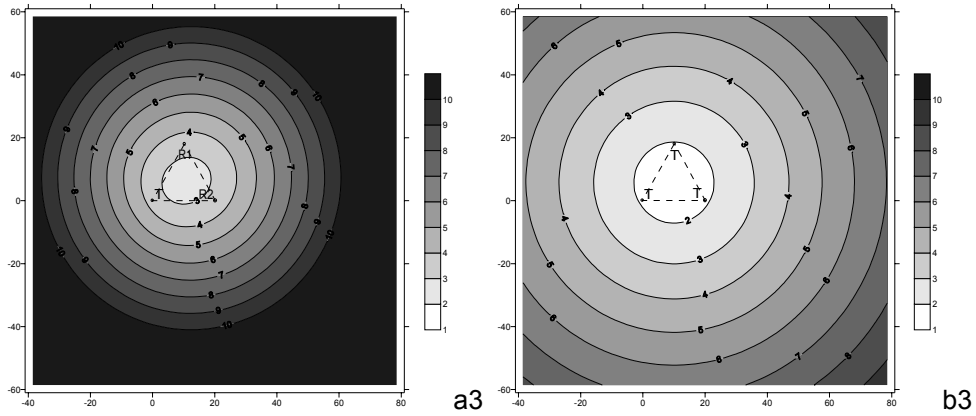

Fig.3. Retrieval precision from 1T-2R observations in a1-a3 *vs* from tri-Doppler radar measurements in b1- b3 at 0, 2.0 and 10.0 km levels, with radars arranged as an equilateral triangle.

Fig.3-a1 delineates the 1T-2R error distribution as an egg-like shape at 0 km level and the symmetry axis through the transmitter is perpendicular to the line connecting two receivers, leading to minimum error inside the area under their joint cover, where error is less than 2 m/s, and away from the joint cover the errors are increased, resulting in a more and more round-looking shape of the distribution.

Figs.3-a2 and 3-a3 present the error distribution at 2 and 10 km level, respectively, indicating that setting 3 m/s to be the acceptable error limit, the surface (0 km) level includes the joint cover and its thereabouts (cf. Fig.3-a1) but the area is on the decrease as a function of height, leading to the retrieval area just inside the joint cover at 10 km level (Fig.3-a3). Obviously, the wind retrieval extent becomes increasingly smaller versus height at the same precision.

Fig.3 (b1-b3) gives the retrieval error distribution at 0, 2 and 10 km levels for the 3 single radar network, leading to the fact that the closer to the radar, the higher precision. Comparing Figs.3a with 3b yields, the accuracy of the former is lower (having the same number of radars) relative to the latter, thereby the retrieval area in the former case is considerably smaller at the same speed measurement accuracy.

To visually compare the extent of the retrieval areas for the two types of radars, Figs.3-a1 and 3-b1 are amplified, as shown in Fig.4.

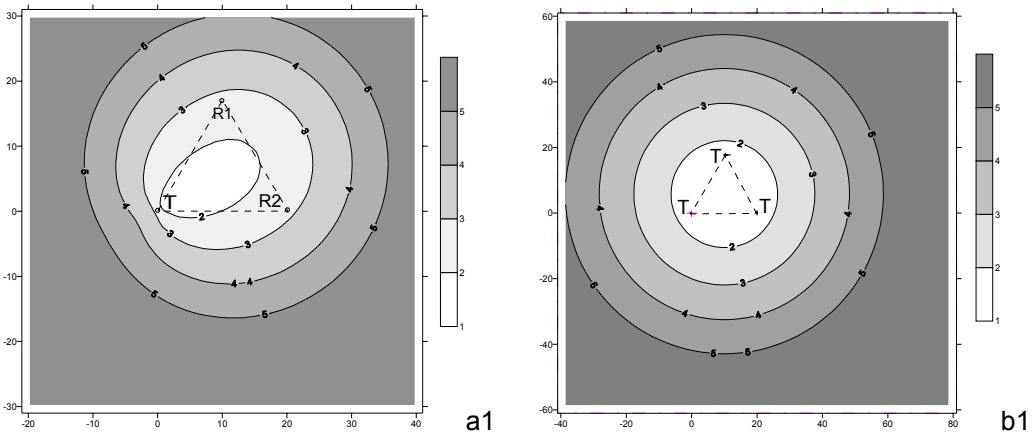

Fig.4. Amplified Fig.3-a1 (1T-2R) vs amplified Fig.3-b1 (tri-Doppler) at 0-km level.

Normally, an area for wind retrieval at errors ≤ 3 m/s is selected for study but here we investigate the extent of an area with errors of ≤ 5 m/s. With variance of ≤ 5 m/s set, and Fig.4 as

example, it is found that the area is as nearly fivefold larger for the tri-Doppler radar network as for 1T-2R, according to rough calculation.

From Fig.4-a1 it is considered that to expand the egg-like joint cover in the bistatic network, the distance between R1 and R2 should be increased, suggesting that the base length (with respect to the apex with the transmitter) of the equilateral triangle is extended to increase the egged shape, thus leading to the initial conclusion that in the bistatic network, the transmitter should be at the apex of the isosceles with the base longer than either of the other side so as to improve believable area.

2.6 The 3D wind Structure and Algorithm for 1T-1R Radars

The 1T-1R results in radial velocity in two directions alone so that we take two equations out of (4) into account, i.e.,

$$\begin{cases} V_{r1} = u\dfrac{\sin a_1 \cos e_1 + \sin a_t \cos e_t}{2\cos(\beta_1/2)} + v\dfrac{\cos a_1 \cos e_1 + \cos a_t \cos e_t}{2\cos(\beta_1/2)} + W\dfrac{\sin e_1 + \sin e_t}{2\cos(\beta_1/2)} \\ V_{rt} = u\sin a_t \cos e_t + v\cos a_t \cos e_t + W\sin e_t \end{cases} \tag{11}$$

which contains 3 unknown quantities, to which is added an expression of mass continuum

$$\frac{\partial u}{\partial x} + \frac{\partial v}{\partial y} + \frac{\partial w}{\partial z} = kw \tag{12}$$

which, put into (11) to form simultaneous equations, permits to find vector winds u, v and W.

2.7 Calculation of 2D Wind Field and Precision Estimation for 1T-1R

The height of target changes little at elevation angle <5°for PPI scanning (Liu et al., 2005), which does not allow to make vertical integral so the effect of vertical velocity on radial speed is ignored at low elevation angles. And in this case (11) is simplified as

$$\begin{cases} V_{r1} = u\dfrac{\sin a_1 \cos e_1 + \sin a_t \cos e_t}{2\cos(\beta_1/2)} + v\dfrac{\cos a_1 \cos e_1 + \cos a_t \cos e_t}{2\cos(\beta_1/2)} \\ V_{rt} = u\sin a_t \cos e_t + v\cos a_t \cos e_t \end{cases} \tag{13a}$$

which contains two unknown variables and as in the case of (5b) the coefficients of *u* and *v* are given by *a* and *b*, respectively, leading to the equations of the form

$$\begin{cases} V_{r1} = a_1 u + b_1 v \\ V_{rt} = a_2 u + b_2 v \end{cases} \tag{13b}$$

whose solutions are in the form

$$\begin{aligned} u &= \frac{V_{r1} b_2 - V_t b_1}{a_1 b_2 - a_2 b_1} \\ v &= \frac{a_1 V_t - a_2 V_{r1}}{a_1 b_2 - a_2 b_1} \end{aligned} \tag{14}$$

Expressions for estimating variance of *u* and *v* are same to (7) and (8), respectively,

$$\sigma_u^2 = (b_1^2 \cdot \sigma_{r1}^2 + b_2^2 \cdot \sigma_{r2}^2)/(a_1 b_2 - a_2 b_1)^2 \tag{15}$$

$$\sigma_v^2 = (a_1^2 \cdot \sigma_{r1}^2 + a_2^2 \cdot \sigma_{r2}^2)/(a_1 b_2 - a_2 b_1)^2 \tag{16}$$

If σ_{hor} is used to denote the standard deviation of horizontal wind, then its expression takes the

same form as (10), viz.,

$$\sigma_{hor} = \sqrt{\sigma_u^2 + \sigma_v^2}$$

Set the transmitter to be the origin of coordinates T (0, 0) and the passive receiver(R) to be 20 km away in the due east of T at R (20, 0). By assuming the same velocity precision of 1 m/s to both the two radars, a 0 – km level diagram is prepared based upon (10) bistatic (1T-1R) horizontal wind retrieval accuracy is calculated (Fig.5a) in comparison to the counterpart for a pair of single radars (Fig.5b).

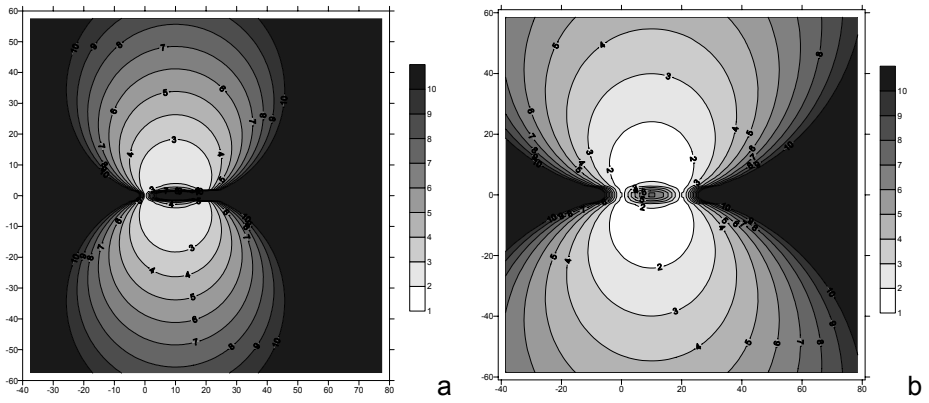

Fig.5. Wind retrieval accuracy from 1T-1R in a) *vs* dual-Doppler radar in b).

Distributions of retrieval errors for 1T-1R and dual-Doppler radar are by way of a circle centered on the bisector of the base line, covering both radar centers, with the base line as the chord of the circle and the farther away from the radar or the closer to the line, the poorer the retrieval accuracy. Comparison shows that in the same arrangement of 1T-1R and dual-Doppler the retrieval precision and extent are lower and smaller, respectively, in the former than in the latter. The maximum retrieval error is 3 m/s for 1T-1R as compared to 2 m/s for dual-Doppler.

2.8 Comparative Study on Wind Retrieval Precision of 1T-2R and 1T-1R

Retrieval precisions for 1T-2R and 1T-1R are presented in sections 2.5 and 2.7, respectively, both differing greatly in distribution (see Figs.3-a1 and 5a).

The 1T-2R arranged in an equilateral triangle shows its retrieval error distribution in an egg-like shape at surface with the symmetry axis passing through the transmitter and perpendicular to the connection between bistatic passive receivers, and high-accuracy retrieval (maximum error of 2 m/s) area is in the center of the enclosure by these radars, indicating that the farther away from the center, the lower the precision. If it is desired to expand the retrieval zone, 1T-2R can be rearranged in a way that puts the transmitter at the apex of the isosceles triangle that has its base longer than any of the other sides.

The retrieval of 1T-1R horizontal wind can reach the highest accuracy of 3 m/s, with its retrieval circular zones symmetric about the base line, which acts as the chord of the circles. Low-precision segment is around and away from the base line.

The observation of 1T-2R radar sounding can be used to make wind retrieval as 1T-2R or 1T-1R network according to requirement.

2.9 Validation of the Algorithm for 2D Wind Retrieval

To test the reliability of 2D wind retrieval and correctness of calculation procedure, numerical modeling is undertaken of wind retrieval based on given 2D wind observations, that is, known radial velocities are given to the active and bistatic passive receivers, followed by use of (13a) and its solution (14) to verify the rationality of the wind retrieval.

Now the particular cases are given as follows: a) V = 0 m/s, and V = 10 m/s; b) V = 10 m/s and V = 0 m/s; c) v = 10 m/s and V = 10 m/s, leading to the vector wind fields as shown in Fig.6. Note that the radars are distributed as in the Hefei field experiment, with the transmitter at the coordinate origin of T(0,0) and the passive being in the east by north by 9.3°, distant 26.8 km from the active and its coordinates being R1 (26.5, 4.3).

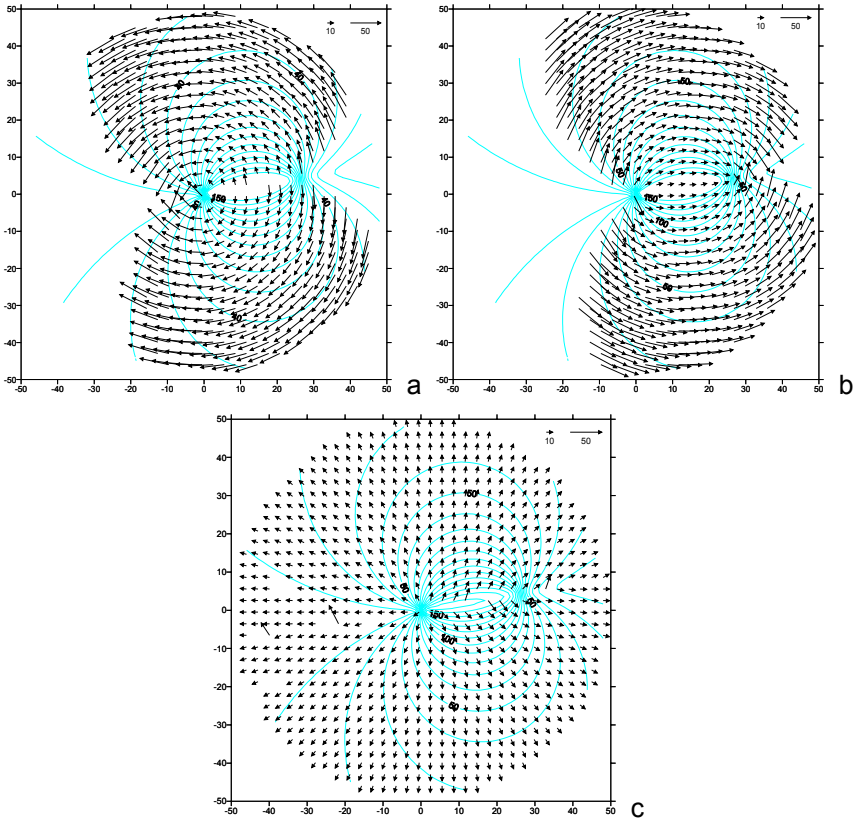

Fig.6. Test of the reliability of the retrieval technique with a) $V_{rt}=0$ and $V_{r1}=10$, b) $V_{rt}=10$ and $V_{r1}=0$ and c) $V_{rt}=10$ and $V_{r1}=10$.

In Fig.6a the transmitter radial velocity V_{rt} = 0 m/s and the passive-receiver-measured radial velocity V_{r1} = 10 m/s. From the retrieval the wind direction is reasonable because the transmitter measured radial velocity is zero and the winds blow just along the tangential of the concentric circles with the transmitter as the core.

Fig.6b is the retrieval at V_{rt} = 10 m/s and V_{r1} = 0 m/s, indicating the wind blows along the tangential of the ellipse family with the transmiter and receiver as the focuses.

Fig.6c depicts the divergent winds symmetric about the base line at V_{rt} = 10 m/s and V_{r1} = 10 m/s.

From these cases, it is clear that the low-precision retrieval zone is in the vicinity of the base line and its extension, where retrieval is hence inappropriate. Note that the contour of bistatic angle β is given in a light-color dotted line.

Based on the limited number of cases assumed to make simulation and calculation, it is found the rationality only of simulated wind direction but nevertheless the technique is applicable although used just in a few cases. In what follows further validation will be made with observations.

3. Application of bistatic wind retrieval

The 1T-2R network developed by Anhui Sun-Create Electron Joint-stock Ltd succeeded in

gaining meteorological echoes in a field operation at Hefei in May and November, 2004. It consists of a transmitter at 3830 C band and two passive radars (as source-free receiver) which were reformed on a synchronous basis.

Based on the data from the 1T-2R positioned in the pattern for experiment in November, 2004, wind retrieval was made, together with error estimate researched.

3.1 The 1T-2R Arrangement for Field Experiment and Retrieval Precision Estimation

This experiment had the 1T-2R distributed, as shown in Fig.7 in an isosceles triangle (see Section 2.5 (Mo, 2005), showing a bigger area for retrieval.

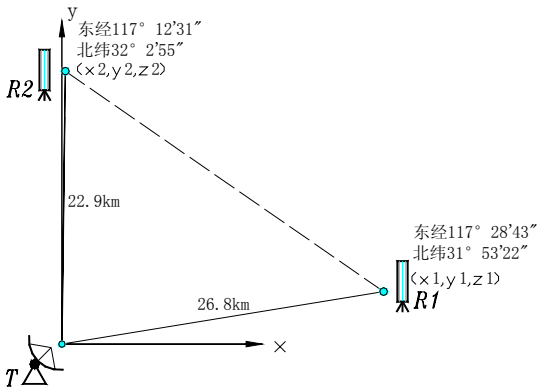

Fig.7. Distribution of 1T-2R radars for Hefei experiment in November of 2004.

When the transmitter sounding is made at a short distance and low elevation angle, the 1T-1R network is used to retrieve horizontal winds (see section 2.7), and the network has probing precision of 1 m/s, with the distribution of retrieval accuracy given in Fig.8.

In Figs.7 and 8 the radar coordinates are T (0,0), R1 (26.5, 4.3) and R2 (1.3, 22.9) and the base line is L_1 = 26.8 and L_2= 22.9 km in Figs.8a and 8b, respectively.

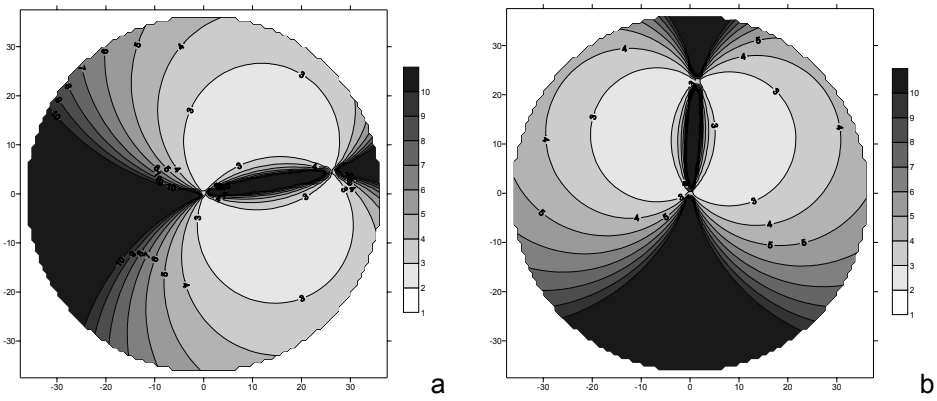

Fig.8. Distribution of ground retrieval precision from 1T-2R data during the field experiment at Hefei, with L_1 = 26.8 km between the transmitter and receiver R1 in a) and L_2 = 22.9 km between the transmitter and receiver R2 in b).

3.2 Example for Wind Retrieval

Pieces of information received by the transmitter and receivers are processed and paired (see Liu et al., 2005; Mo, 2005) to guarantee the echoes indeed from the same time and target, followed by data preprocessing, e.g., data quality control and data for interpolation before calculating the 3D wind by means of equations (5a).

Data quality control refers mainly to data checking to remove points of wrong data, noise, supplement of missing data, coordinate transformation and filtering and point interpolation. The

filtered data are interpolated at a 0.5 km×0.5 km grid.

For low elevation angles and smaller-size measurement, 2D horizontal wind retrieval is made by (13a) on the PPI.

The retrieval case is selected of light – moderate stratiform precipitation at Hefei on November 9, 2004. Figs.9 and 10 show the retrieval on the PPI at 1647 and 1708 BT (Beijing Time), respectively, with a and b indicating the transmitter received echo intensity and measured radial velocity, respectively and c giving the bistatic retrieval. To better investigate the distribution of radial velocity in relation to winds, a chart of transmitter radial velocity subject was superimposed on retrieval for quality control. Moreover, a bistatic angle β contour is superimposed on the wind field to limit the bistatic retrieval area.

Studies on 1T-1R retrieval error in relation to the bistatic angle β arrive at a conclusion that the area of errors smaller than 3% is within the bound of 40°<β< 150°(Satoh and Wurman, 2003; Mo, 2005), suggesting that the precision is warranted only in this interval, with maximal accuracy at β≈100°. The retrieval sector within such a bound in Figs.9 and 10 is too small to discern the wind direction so that the bottom limit of the bistatic angle is set to be β=30°.

As shown in Fig.9b for radial velocity, winds passing the radar station are southwest, which no such wind is detected in the due south just because of screening effect around the station (Mo, 2005; Mo et al., 2005), with little change in direction but speed increase as a function of height (winds are stronger at the same place in Fig.9 relative to Fig.10). The bistatic retrievals indicate that the retrievable area is dominated by southwest winds, exhibiting height-dependent wind intensification as well, so the conclusion agrees with analysis aforementioned, implying that the retrieval method is viable.

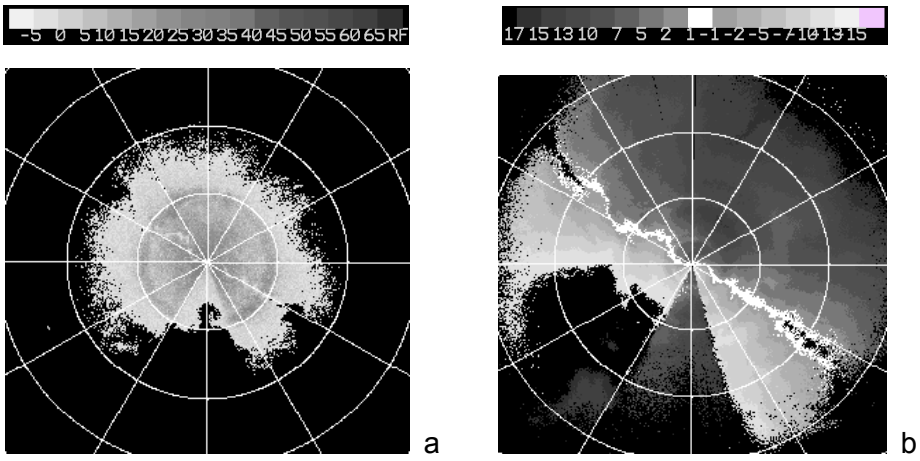

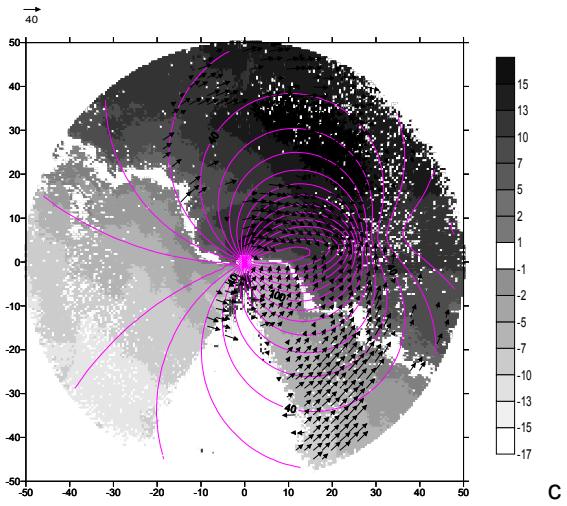

Fig.9. Example for retrieval at the transmitter elevation e = 4.7°, at 1647 BT, November 9, 2004 at Hefei, with transmitter primitive echo intensity in a), its radar blind area of raw radial velocity due to nearby screening in the due south in b), wind retrievals from bistatic measurements, showing superimposition on the retrievals a chart of radial velocity subject to the quality control, with the length of arrows indicative of the wind force as well as dashed line denoted bistatic angle β contour in c).

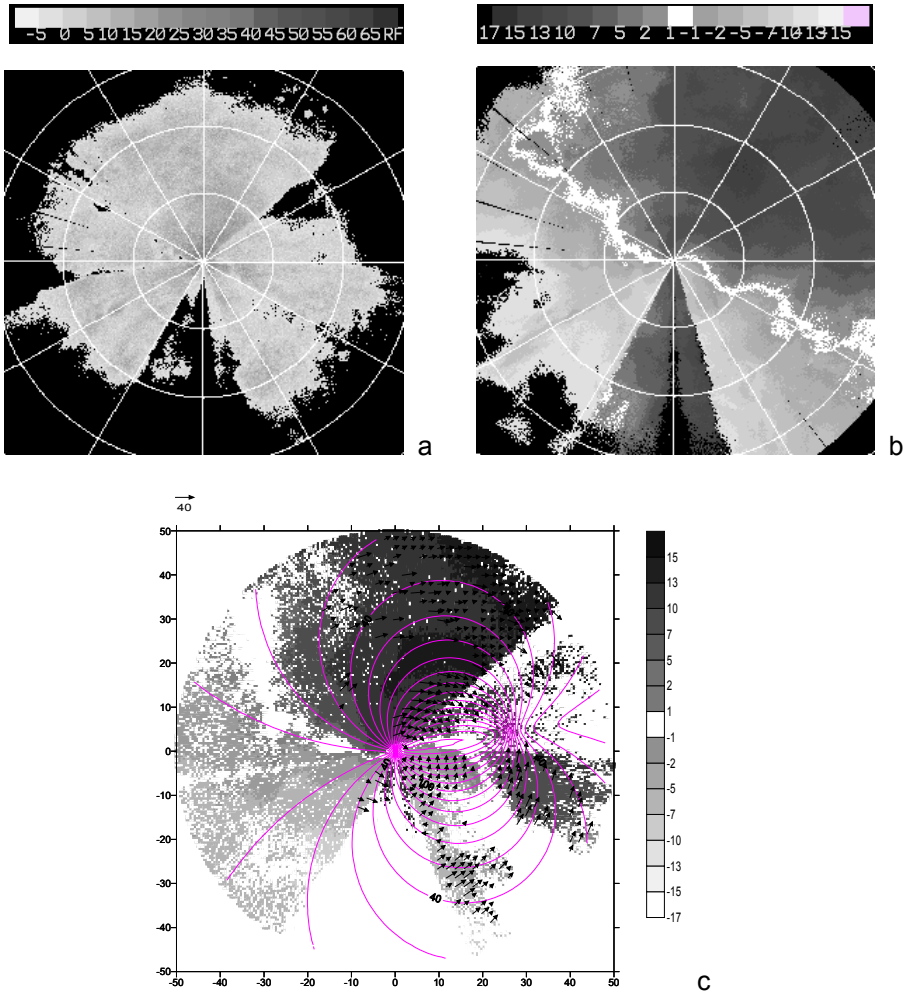

Fig.10. as in Fig.9 except for e = 4.13°at 1708 BT.

Additionally, it is apparent from these figures that in the zero radial velocity zone of the transmitter the retrieved wind is perpendicular to radar beam, thereby they are harmony.

With the radar arrangement as shown in Fig.7, the valid zone for retrieval from transmitter T and bistatic receiver R1 data is a band of 40 km×35 km on either side of the base line, which covers most of the bound 40°<β<150°(refer to Fig.11).

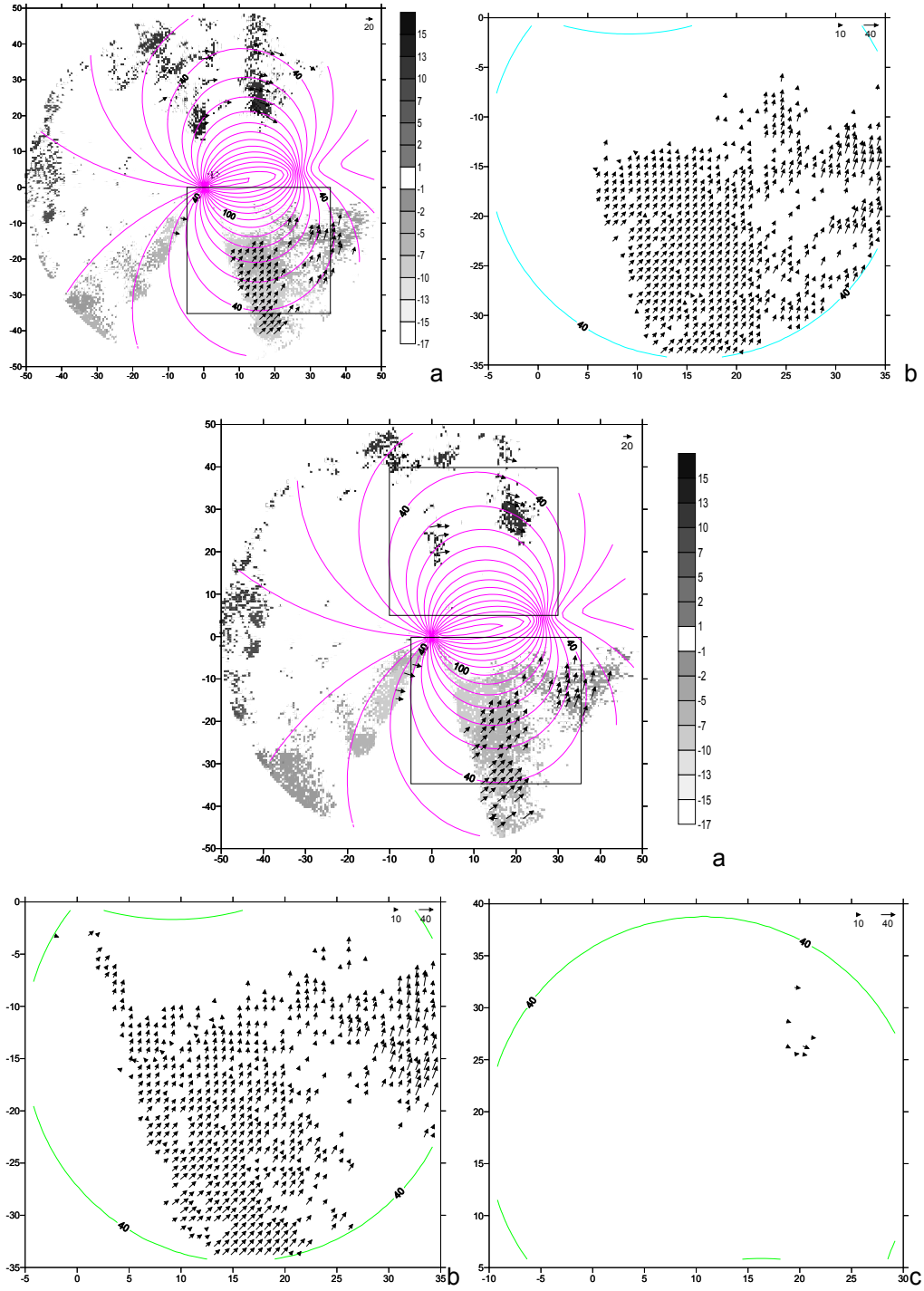

Fig.11. Estimated wind retrieval zone at elevation e =4.7°and e = 3.54°for the transmitter at 1414 and 1417 BT, respectively, on November 9, 2004, with retrievals superimposed on by quality-control-treated transmitter radial velocities and the winds imposed on by a bistatic angleβ contour (dashed line) is showed in a), the southern and northern partial retrieval zone amplified are in b) and c), respectively.

Obviously, if the bistatic network distribution were utterly uniform to the arrangement in Fig.7, the requirement of wind retrieval precision can be satisfied without considering the bistatic angle but setting the retrieval zone in an area which is 40 km×35 km on both sides of the base line, and by doing that the computational cost can be greatly decreased. Actually, if the bistatic radar distribution is arranged and the retrieval zone is clear, the wind field retrieval can be achieved on required

precision.

4. Discussion and conclusions

Based on wind retrieval from multiple Doppler radars data, a retrieval method is established for a bistatic Doppler radar network by using a wind vector compositing technique, and also the estimation of retrieval precision is made, which is compared to the accuracy of retrieval from single site radars measurements. Besides, wind retrieval and precision analysis are performed from the measurement of the field experiments at Hefei with a bistatic-multiple radar network developed by Anhui Sun-Create Electron Ltd.. The following conclusions are arrived.

1) Numerical modeling and calculation are made by using the bistatic 2D wind algorithm, the results indicate the technique presented here is rational.

2) To 1T-2R distributed as an equilateral triangle, in which all the radars have 1 m/s precision in measuring velocity, the retrieval errors are distributed in an egg-like shape where the minimal error is located in the zone under joint cover of the three radars, and errors increased outward. Compared to a network of three single-base radars, the bistatic effective retrieval zone is smaller and the retrieval area can be expanded to some degree if the 1T-2R network is arranged as an isosceles triangle with the transmitter at the apex and the base longer than either of the other sides.

3) The 1T-1R retrieval error distribution is a circle centered on the bisector of the base line, which covers both the two radars. The farther away from the radars or closer to the base line the position is, the lower retrieval precision there is.

4) The form of the error distribution for 1T-2R differs greatly from that for 1T-1R, and the retrieval precision is higher but retrievable zone is smaller in the former. The 1T-2R data can be used to make wind retrieval as data from 1T-2R or 1T-1R.

5) Through the measurement-based retrieval, it is discovered that in the zone where zero radial velocity detected by the active radar, by using bistatic network data the velocity component perpendicular to transmitter beam can still be retrieved. Thus it is suggested that the bistatic soundings can serve as the effective supplement to single-base probing.

6) To sum up, though bistatic wind retrieval extent and retrieval accuracy are inferior to those from data provided by single-base-radar network, it can be used in retrieving fine-structured wind and used in small-scale key region retrieval. As the bistatic radars positioned in Fig.7, a reliable vector wind field over 40 km×35 km band on either side of the base line can be got. Particularly in the case of low investment, its principle of lateral probing can be utilized to remedy deficits of single radar network. The bistatic radar network can achieve higher output – input ratio.

Acknowledgment. The authors are grateful to Wei Moran, a student of Zhejiang University, for drawing some figures and running computer program.

REFERENCES

Armijo, L., 1969: A theory for the determination of wind and precipitation velocities with Doppler radars, *J. Atmos. Sci.*, **26**, 570-573.

Atlas, D., K. Naito, and R. E. Carbone, 1968: Bistatic microwave probing of a refractively perturbed clear atmosphere, *J. Atmos. Sci.*, **25,** 257-268.

Doviak, R. J., and C. M. Weil, 1972: Bistatic radar detection of the melting layer, *J. Appl. Meteor.*, **11**, 1012-1016.

Kong, F. Y., and J. T. Mao, 1994: A model study of three-dimensional wind field analysis from dual-doppler radar data. Advances in Atmospheric Sciences, **11**: 162-174.

Liu, L. P., Y. Q. Mo, T. Su, and X. S. Sha, 2005: Radar Data Processing and a Variational Algorithm for 3-Dimensional Wind Field Retrieval by C Band Bistatic Radar Network, *Chinese J. of Atmospheric Sciences,* **30** (6) (in Chinese).

Liu, L. P., P. Y. Zhang, H. H. Liang, and H. G. Zhou, 2003: Error Estimation in Wind Fields Derived from Dual-Doppler Radar and Data Quality Control, *Quarterly J. of Applied. Meteor*, **14** (1), 17-19 (in Chinese).

Liu, L. P., P. F. Zhang，X. Qin，F. Y. Kong，and S. Liu，2005: A model for retrieval of dual linear polarization radar fields from model simulation outputs. Advances in Atmospheric Sciences，**22**, 711-719.

Mo, Y. Q., L. P. Liu, B. X. Xu, T. Su, and X. S. Sha, 2005: Detecting Capability Analysis on a Bistatic Doppler Radar Network, *Acta Meteor. Sinica,* **63** (6), 994-1005 (in Chinese).

Mo, Y. Q., 2005: The Study of Probing Theory and Application Analysis of Bistatic Doppler Weather Radar, presented at NUIST as her Ph. D. thesis under the joint direction of NUIST and CAMS (in Chinese).

Protat, A., and I. Zawadzki, 1999: A variational method for real-time retrieval of three-dimensional wind field from multiple- bistatic Doppler radar network data, *J. Atmos. And Oceanic Tech*., **16** (4), 432-449.

Qiu, C. J., and Q.Xu , 1996: Least squares retrieval of microburst from single Doppler data, *Mon. Wea. Rev.*, **124**, 1132-1144.

Ray, P. S., C. L. Zirgler, and R. J. Serafin, 1980: Single- and multi-Doppler radar observations of tornadic storms, *Mon. Wea, Rev.*, **108**,1607-1625.

Satoh, S. and j. Wurman, 2003: Accuracy of wind fields observed by a bistatic Doppler radar network, *J. Atmos. And Oceanic Tech*. **20**, 1077-1091.

Skolnik, Merrill I., 2003: Radar Handbook (2nd edition), translated by Wang Jun, Lin Qiang, Mi Cizhong et al., China Electronic Industry Press, Beijing, 1018 pp. (in Chinese).

Wurman, J., S. Heckman, and D. Boccippio, 1993: A bistatic multiple-radar network, *J. Appl. Meteor*., **32** (7-12), 1802-1814.

Xu, H., W. P. Zhang, X. X. Lang, X. Guo, W. Z. Ge, R. Q. Dang, and T. Akao, 2000: The use of dual-doppler radar data in the study of 1998 meiyu frontal precipitation in huaihe river basin. Advances in Atmospheric Sciences, **17**, 403-412.

Yang, Z. Q., Y. S. Zhang, and Y. J. Luo, 2001: Bistatic-Multiple Doppler Radar Systems, China National Defense Press, Beijing, 289 pp. (in Chinese).

Zhang, P. Y., P. He, C. M. Song, and R. S. Ge, 1998: A Study on Error Distribution and Radar Optimum Arrangements of Wind Field Measurement with Doppler Radars, *Acta Meteor. Sinica*, **56**(1), 96-103 (in Chinese).

Zhou, H. G., and Y. B. Wang, 2003: Contrastive Study on Three-Dimensional Wind Field of Mei-yu Precipitation using Dual-and Triple-Doppler Radar, *Meteorological Monthly*.，**29**(5), 13-17 (in Chinese).

Zhou, H. G., and P. Y. Zhang, 2002: A New Technique of Recovering Three-dimensional Wind Fields from Simulated Dual-Dopler Radar Data in the Cartesian Space. *Acta Meteor. Sinica*, **60**(5), 585-593 (in Chinese).